

BEST AVAILABLE COPY

1260772

UNITED STATES PATENT AND TRADEMARK OFFICE

TO ALL TO WHOM THESE PRESENTS SHALL COME:

UNITED STATES DEPARTMENT OF COMMERCE

United States Patent and Trademark Office

December 13, 2004

THIS IS TO CERTIFY THAT ANNEXED HERETO IS A TRUE COPY FROM
THE RECORDS OF THE UNITED STATES PATENT AND TRADEMARK
OFFICE OF THOSE PAPERS OF THE BELOW IDENTIFIED PATENT
APPLICATION THAT MET THE REQUIREMENTS TO BE GRANTED A
FILING DATE.

APPLICATION NUMBER: 60/546,174
FILING DATE: *February 23, 2004*
RELATED PCT APPLICATION NUMBER: PCT/US04/35143

Certified by



Jon W Dudas

Acting Under Secretary of Commerce
for Intellectual Property
and Acting Director of the U.S.
Patent and Trademark Office





13281 U.S.PTO

Page 1 of 2

IN THE UNITED STATES PATENT AND TRADEMARK OFFICE

REQUEST FOR FILING PROVISIONAL PATENT APPLICATION

Under 35 USC 111(b)
 (Not for DESIGN cases)

Box: PROVISIONAL
APPLICATION

The Asst. Commissioner of Patents
and Trademarks
Washington, D.C. 20231

PROVISIONAL APPLICATION
Under Rule 53(c)

22141 U.S.PTO
60/546174

Sir:

Herewith is a PROVISIONAL APPLICATIONTitle: SPECTRAL IDENTIFICATION OF NEW STATES OF
HYDROGEN BY VIBRATION-ROTATIONAL
SPECTROSCOPY

Our Order No.	62226	
50-0687	C#	M#
Atty. Dkt.	62226-P-HLAS2	
	M#	Client Ref

including:

Date: February 23, 2004

1. Specification: 23 pages 2. Specification in non-English 3. Drawings: 9 sheet(s)4. The invention was was not made by, or under a contract with, an agency of the U.S. Government.

If yes, Government agency/contact # = _____

5. Attached is an assignment and cover sheet. Please return the recorded assignment to the undersigned.6. Applicant(s) claims "small entity" status under Rules 9 & 27.7. Attached:

8. This application is made by the following named inventor(s) (Double check instructions for accuracy.):

(1) Inventor	Randell	L.	Mills
	First	Middle Initial	Family Name
Residence	Cranbury		New Jersey
	City		State/Foreign Country

(2) Inventor			
	First	Middle Initial	Family Name
Residence			
	City		State/Foreign Country

(3) Inventor			
	First	Middle Initial	Family Name
Residence			
	City		State/Foreign Country

(4) Inventor			
First		Middle Initial	Family Name
Residence			
City		State/Foreign Country	

(5) Inventor			
First		Middle Initial	Family Name
Residence			
City		State/Foreign Country	

	Large/Small Entity		Fee Code
10. Filing Fee	\$80	\$ 80	114/214
11. If "non-English" box 2 is X'd, add Rule 17(k) processing fee	\$	+	139
12. If "assignment" box 5 is X'd, add recording fee	\$		581
13.	TOTAL FEE ENCLOSED =		\$80

CHARGE STATEMENT: The Commissioner is hereby authorized to charge any fee specifically authorized hereafter, or any missing or insufficient fee(s) filed, or asserted to be filed, or which should have been filed herewith or concerning any paper filed hereafter, and which may be required under Rules 16-17 (missing or insufficient fee only) now or hereafter relative to this application or credit any overpayment, to our Account/Order Nos. shown in the heading hereof for which purpose a duplicate copy of this sheet is attached.

Manelli Denison & Selter,
PLLC

By: Atty: **Jeffrey S. Melcher**

Reg.
No. **35,950**

Customer No.: 20736

Sig: 

Fax: (202) 887-0336

Tel: (202)261-1045

NOTE: File in duplicate with 2 post card receipts & attachments

APPLICATION UNDER UNITED STATES PATENT LAWS

Invention: SPECTRAL IDENTIFICATION OF NEW STATES OF HYDROGEN BY VIBRATION-ROTATIONAL SPECTROSCOPY

**Inventor(s): Randell L. Mills
493 Old Trenton Road
Cranbury, New Jersey 08512**

Attorney Docket No: 62226-P-HLAS2

**Jeffrey S. Melcher
Manelli, Denison & Selter P.L.L.C.
Customer No.: 20736
2000 M Street, N.W.
7th Floor
Washington, D.C. 20036-3307**

THIS IS A PROVISIONAL PATENT APPLICATION

SPECIFICATION



13281 U.S.PTO
022304

Spectral Identification of New States of Hydrogen by Vibration-Rotational Spectroscopy

R. L. Mills, Y. Lu, B. Dhandapani
BlackLight Power, Inc., 493 Old Trenton Road, Cranbury, NJ 08512

ABSTRACT

Novel emission lines with energies of $q \cdot 13.6 \text{ eV}$ where $q = 1, 2, 3, 4, 6, 7, 8, 9, \text{ or } 11$ were previously observed by extreme ultraviolet (EUV) spectroscopy recorded on microwave discharges of helium with 2% hydrogen [R. L. Mills, P. Ray, J. Phys. D, Applied Physics, Vol. 36, (2003), pp. 1535-1542]. These lines matched $H(1/p)$, fractional Rydberg states of atomic hydrogen wherein $n = \frac{1}{2}, \frac{1}{3}, \frac{1}{4}, \dots, \frac{1}{p}$; ($p \leq 137$ is an integer) replaces the well known parameter

$n = \text{integer}$ in the Rydberg equation for hydrogen excited states. Evidence supports that these states are formed by a resonant nonradiative energy transfer to He^+ acting as a catalyst. Ar^+ also serves as a catalyst to form $H(1/p)$; whereas, krypton, xenon, and their ions serve as controls. Two $H(1/p)$ may react to form $H_2(1/p)$ that have vibrational and rotational energies that are p^2 times those of the species comprising uncatalyzed atomic hydrogen. Rotational lines were observed in the 145-185 nm region from atmospheric pressure electron-beam excited argon-hydrogen plasmas. The unprecedented energy spacing of 4^2 times that of hydrogen established the internuclear distance as 1/4 that of H_2 and identified $H_2(1/4)$. The Doppler shifted energies, Gaussian peak shapes, Doppler widths, and intensities of the predicted vibration-rotational emission of $D_2(1/4)$ comprising P(1) and P(3) peaks were observed that identified $D_2(1/4)$, a deuterium molecule with an internuclear distance of 1/4 that of ordinary D_2 . The observation of the predicted vibration-rotation spectra for both isotopes provides substantial evidence for the existence of new states of hydrogen formed by a catalytic plasma reaction.

Keywords: fractional-principal-quantum-level atomic and molecular hydrogen, vibration-rotational series, deuterium substitution

I. Introduction

A. Theoretical Predictions

The basic spectral emission of pure helium and hydrogen light sources have been well known for about a century. Recently, however, unique EUV emission lines were found at predicted wavelengths and reported in numerous publications [1-5]. For example, EUV spectroscopy was recorded on microwave discharges of helium with 2% hydrogen. Novel emission lines were observed with energies of $q \cdot 13.6 \text{ eV}$, $q = 1, 2, 3, 7, 9, 11$, or $q \cdot 13.6 \text{ eV}$, $q = 4, 6, 8$ less 21.2 eV corresponding to inelastic scattering of these photons by helium atoms due to excitation of $\text{He}(\text{1s}^2)$ to $\text{He}(\text{1s}^1\text{2p}^1)$. These strong emissions are not found in any single gas plasma, and cannot be assigned to the known emission of any species of the single gases studied such as H , H^- , H_2 , H_2^+ , H_3^+ , He , He_2^+ , and He^+ , known species of the mixture such as He_2^+ , HeH^+ , HeH , HHe_2^+ , and HHe_n^+ and He_n , or possible contaminants [1]. However the results can be explained by a novel catalytic reaction involving atomic hydrogen [1-5].

J. R. Rydberg showed that all of the spectral lines of atomic hydrogen were given by a completely empirical relationship:

$$\bar{\nu} = R \left(\frac{1}{n_f^2} - \frac{1}{n_i^2} \right) \quad (1)$$

where $R = 109,677 \text{ cm}^{-1}$, $n_f = 1, 2, 3, \dots$, $n_i = 2, 3, 4, \dots$ and $n_i > n_f$. Bohr, Schrödinger, and Heisenberg each developed a theory for atomic hydrogen that gave the energy levels in agreement with Rydberg's equation.

$$E_n = -\frac{e^2}{n^2 8\pi\epsilon_0 a_H} = -\frac{13.598 \text{ eV}}{n^2} \quad (2a)$$

$$n = 1, 2, 3, \dots \quad (2b)$$

where e is the elementary charge, ϵ_0 is the permittivity of vacuum, and a_H is the radius of the hydrogen atom. The excited energy states of atomic hydrogen are given by Eq. (2a) for $n > 1$ in Eq. (2b). The $n = 1$ state is the "ground" state for "pure" photon transitions (i.e. the $n = 1$ state can absorb a photon and go to an excited electronic state, but it cannot release a photon and go to a lower-energy electronic state). However, an electron transition from the ground state to a lower-energy state may be possible by a resonant nonradiative energy transfer such as multipole coupling or a resonant collision mechanism. Processes such as hydrogen molecular bond formation that occur without photons and that require collisions are common [6]. Also, some commercial phosphors are based on resonant nonradiative energy transfer involving multipole coupling [7].

The theory reported previously [1-5, 8-13] predicts that atomic hydrogen may undergo a catalytic reaction with certain atoms, excimers, and ions which provide a reaction with a net enthalpy of an integer multiple of the potential energy of atomic hydrogen, $E_h = 27.2 \text{ eV}$ where E_h is one hartree. Specific species (e.g. He^+ , Ar^+ , and K) identifiable on the basis of their known electron energy levels are required to be present in plasmas with atomic hydrogen to catalyze the process. In contrast, species such as atoms or ions of Kr or Xe do not fulfill the catalyst criterion—a chemical or physical process with an enthalpy change equal to an integer multiple of E_h that is sufficiently reactive with atomic hydrogen under reaction conditions. The reaction involves a nonradiative energy transfer followed by $q \cdot 13.6 \text{ eV}$ emission or $q \cdot 13.6 \text{ eV}$ transfer to H to form extraordinarily hot, excited-state H [11-17], and a hydrogen atom that is lower in energy than unreacted atomic hydrogen that corresponds to a fractional principal quantum number. That is

$$n = \frac{1}{2}, \frac{1}{3}, \frac{1}{4}, \dots, \frac{1}{p}; \quad p \leq 137 \text{ is an integer} \quad (2c)$$

replaces the well known parameter $n = \text{integer}$ in the Rydberg equation for hydrogen excited states. The $n = 1$ state of hydrogen and the $n = \frac{1}{\text{integer}}$ states of hydrogen are nonradiative, but a transition between two nonradiative states, say $n = 1$ to $n = 1/2$, is possible via a nonradiative energy transfer. Thus, a catalyst provides a net positive enthalpy of reaction of $m \cdot 27.2 \text{ eV}$ (i.e. it resonantly accepts the nonradiative energy transfer from hydrogen atoms and releases the energy to the surroundings to affect electronic transitions to fractional quantum energy levels). As a consequence of the nonradiative energy transfer, the hydrogen atom becomes unstable and emits further energy until it achieves a lower-energy nonradiative state having a principal energy level given by Eqs. (2a) and (2c).

Prior related studies that support the possibility of a novel reaction of atomic hydrogen which produces hydrogen in fractional quantum states that are at lower energies than the traditional “ground” ($n = 1$) state include EUV spectroscopy [1-5, 10-13, 16-27], characteristic emission from catalysts and the hydride ion products [12-13, 18-20, 22-23], lower-energy hydrogen emission [1-5], chemically formed plasmas [10-13, 18-23], Balmer α line broadening [1, 2, 11-18, 20, 22-23, 25-26], population inversion of H lines [22-25], elevated electron temperature [14-16, 26], anomalous plasma afterglow duration [21], power generation [2, 4, 16, 20, 26], and analysis of novel chemical compounds [20, 28-30].

$H(1/p)$ may react with a proton and two $H(1/p)$ may react to form $H_2(1/p)^+$ and $H_2(1/p)$, respectively. The hydrogen molecular ion and molecular charge and current density functions, bond distances, and energies were solved previously [9] from the Laplacian in ellipsoidal coordinates with the constraint of nonradiation.

$$(\eta - \zeta)R_\xi \frac{\partial}{\partial \xi} (R_\xi \frac{\partial \phi}{\partial \xi}) + (\zeta - \xi)R_\eta \frac{\partial}{\partial \eta} (R_\eta \frac{\partial \phi}{\partial \eta}) + (\xi - \eta)R_\zeta \frac{\partial}{\partial \zeta} (R_\zeta \frac{\partial \phi}{\partial \zeta}) = 0 \quad (3)$$

The total energy of the hydrogen molecular ion having a central field of $+pe$ at each focus of the prolate spheroid molecular orbital is

$$E_T = -p^2 \left\{ \frac{e^2}{8\pi\epsilon_0 a_H} (4\ln 3 - 1 - 2\ln 3) \left[1 + p \sqrt{2\hbar \sqrt{\frac{2e^2}{4\pi\epsilon_0 (2a_H)^3}} \frac{m_e}{m_e c^2}} \right] - \frac{1}{2} \hbar \sqrt{\frac{k}{\mu}} \right\}$$

$$= -p^2 16.13392 \text{ eV} - p^3 0.118755 \text{ eV} \quad (4)$$

where p is an integer, \hbar is Planck's constant bar, m_e is the mass of the electron, c is the speed of light in vacuum, μ is the reduced nuclear mass, and k is the harmonic force constant solved previously [9]. The total energy of the hydrogen molecule having a central field of $+pe$ at each focus of the prolate spheroid molecular orbital is

$$E_T = -p^2 \left\{ \frac{e^2}{8\pi\epsilon_0 a_0} \left[\left(2\sqrt{2} - \sqrt{2} + \frac{\sqrt{2}}{2} \right) \ln \frac{\sqrt{2}+1}{\sqrt{2}-1} - \sqrt{2} \right] \left[1 + p \sqrt{2\hbar \sqrt{\frac{e^2}{4\pi\epsilon_0 a_0^3}} \frac{m_e}{m_e c^2}} \right] - \frac{1}{2} \hbar \sqrt{\frac{k}{\mu}} \right\}$$

$$= -p^2 31.351 \text{ eV} - p^3 0.326469 \text{ eV} \quad (5)$$

where a_0 is the Bohr radius.

The bond dissociation energy, E_D , of hydrogen molecular ion $H_2(1/p)^+$ is the difference between the total energy of the corresponding hydrogen atom $H(1/p)$ and E_T :

$$E_D = E(H(1/p)) - E_T \quad (6)$$

where [31]

$$E(H(1/p)) = -p^2 13.59844 \text{ eV} \quad (7)$$

E_D is given by Eqs. (6-7) and Eq. (4):

$$\begin{aligned} E_D &= -p^2 13.59844 - E_T \\ &= -p^2 13.59844 - (-p^2 16.13392 \text{ eV} - p^3 0.118755 \text{ eV}) \\ &= p^2 2.535 \text{ eV} + p^3 0.118755 \text{ eV} \end{aligned} \quad (8)$$

The bond dissociation energy, E_D , of hydrogen molecule $H_2(1/p)$ is the difference between the total energy of the corresponding hydrogen atoms and E_T

$$E_D = E(2H(1/p)) - E_T \quad (9)$$

where [31]

$$E(2H(1/p)) = -p^2 27.20 \text{ eV} \quad (10)$$

E_D is given by Eqs. (9-10) and (5):

$$\begin{aligned} E_D &= -p^2 27.20 \text{ eV} - E_T \\ &= -p^2 27.20 \text{ eV} - (-p^2 31.351 \text{ eV} - p^3 0.326469 \text{ eV}) \\ &= p^2 4.151 \text{ eV} + p^3 0.326469 \text{ eV} \end{aligned} \quad (11)$$

The calculated and experimental parameters of H_2 , D_2 , H_2^+ , and D_2^+ from Ref. [9] are given in Table 1.

The vibrational and rotational energies of fractional-Rydberg-state hydrogen molecular ion $H_2(1/p)^+$ and molecular hydrogen $H_2(1/p)$ are p^2 those of H_2^+ and H_2 , respectively. Thus, the vibrational energies, E_{vib} , for the $\nu = 0$ to $\nu = 1$ transition of hydrogen-type molecular ions $H_2(1/p)^+$ are [9]

$$E_{vib} = p^2 0.271 \text{ eV} \quad (12)$$

where p is an integer and the experimental vibrational energy for the $\nu = 0$ to $\nu = 1$ transition of H_2^+ , $E_{H_2^+ (\nu=0 \rightarrow \nu=1)}$, is given by Karplus and Porter [32] and NIST [33]. Similarly, the rotational energy levels are given by [34]

$$E_{rotational} = \frac{\hbar^2}{2I} J(J+1) \quad (13)$$

and the rotational energies, E_{rot} , for the J to $J+1$ transition of hydrogen-type molecular ions $H_2(1/p)^+$ are [9]

$$E_{rot} = E_{J+1} - E_J = \frac{\hbar^2}{I} [J+1] = p^2 (J+1) 0.00739 \text{ eV} \quad (14)$$

where J is an integer, I is the moment of inertia, p is an integer corresponding to $H_2(1/p)^+$, and the experimental rotational energy for the $J = 0$ to $J = 1$ transition of H_2^+ is given by Atkins [35].

The vibrational energies, E_{vib} , for the $\nu = 0$ to $\nu = 1$ transition of hydrogen-type molecules $H_2(1/p)$ are [9]

$$E_{vib} = p^2 0.515902 \text{ eV} \quad (15)$$

where p is an integer and the experimental vibrational energy for the $\nu = 0$ to $\nu = 1$ transition of H_2 , $E_{H_2 (\nu=0 \rightarrow \nu=1)}$, is given by Beutler [36] and Herzberg [37].

Similarly to $H_2(1/p)^+$, the rotational energies, E_{rot} , for the J to $J+1$ transition of hydrogen-type molecules $H_2(1/p)$ are [9]

$$E_{rot} = E_{J+1} - E_J = \frac{\hbar^2}{I} [J+1] = p^2 (J+1) 0.01509 \text{ eV} \quad (16)$$

where p is an integer, I is the moment of inertia, and the experimental rotational energy for the $J = 0$ to $J = 1$ transition of H_2 is given by Atkins [35].

The p^2 dependence of the rotational energies results from an inverse p dependence of

the internuclear distance and the corresponding impact on I . The predicted internuclear distances $2c'$ for $H_2(1/p)^+$ and $H_2(1/p)$ are

$$2c' = \frac{2a_0}{p} \quad (17)$$

and

$$2c' = \frac{a_0\sqrt{2}}{p} \quad (18)$$

respectively.

The reaction Ar^+ to Ar^{2+} has a net enthalpy of reaction of 27.63 eV; thus, it may serve as a catalyst to form $H(1/2)$. The product of the catalysis reaction, $H(1/2)$, may further serve as both a catalyst and a reactant to form $H(1/4)$ [2-3]. Also, the second ionization energy of helium is 54.4 eV; thus, the ionization reaction of He^+ to He^{2+} has a net enthalpy of reaction of 54.4 eV which is equivalent to $2 \cdot 27.2$ eV. The product of the catalysis reaction, $H(1/3)$, may further serve as both a catalyst and a reactant to form $H(1/4)$ and $H(1/2)$ [2-3].

Since $H_2(1/2)^+$ is a resonant state of $H_2(1/4)^+$, the reaction designated



wherein $H(1/4)$ reacts with a proton to form $H_2(1/4)^+$ is possible with strong emission through vibronic coupling with the resonant state $H_2(1/2)^+$. As given previously [9], the energies, E_{D+vib} , of this series due to vibration in the transition state are given by

$$\begin{aligned} E_{D+vib} &= E_D(H_2(1/4)^+) - \left(v^* + \frac{1}{2}\right) 2^2 E_{vib H_2^+}, \quad v^* = 0, 1, 2, 3, \dots \\ &= 48.16 - \left(v^* + \frac{1}{2}\right) 1.172 \text{ eV} \end{aligned} \quad (20)$$

where $E_D(H_2(1/4)^+)$ is the bond energy of $H_2(1/4)^+$ given by Eq. (8) and $E_{vib H_2^+}$ is the transition-state vibrational energy of H_2^+ given by

$$E_{vib} = \hbar\omega = \hbar p^2 4.44865 \times 10^{14} \text{ rad/s} = p^2 0.2928 \text{ eV} \quad (21)$$

In Eq. (20), v^* refers to vibrational energies of the transition state which must have equal energy separation as a requirement for resonant emission [9]. Thus, anharmonicity is not predicted. The series is predicted to end at 25.74 nm corresponding to the predicted $H_2(1/4)^+$ bond energy of 48.16 eV given by Eq. (8). A series of over twenty peaks in the 10-65 nm region emitted from low-pressure helium-hydrogen (90/10%) and argon-hydrogen (90/10%) microwave plasmas matched the energy spacing of 2^2 times the transition-state vibrational energy of H_2^+ with the series ending on the bond energy of $H_2(1/4)^+$ [38].

$H_2(1/p)$ gas was isolated by liquefaction at liquid nitrogen temperature and by decomposition of compounds found by 1H MAS NMR to contain the corresponding hydride ions $H^-(1/p)$. The $H_2(1/p)$ gas was dissolved in $CDCl_3$ and characterized by 1H NMR.

Considering solvent effects, singlet peaks upfield of H_2 were observed with a predicted integer spacing of 0.64 ppm at 3.47, 3.02, 2.18, 1.25, 0.85, and 0.22 ppm which matched the consecutive series $H_2(1/2)$, $H_2(1/3)$, $H_2(1/4)$, $H_2(1/5)$, $H_2(1/6)$, and $H_2(1/7)$, respectively.

The exothermic helium plasma catalysis of atomic hydrogen was shown previously [14-15] by the observation of an average hydrogen atom temperature of 180 - 210 eV for helium-hydrogen mixed plasmas versus ≈ 3 eV for hydrogen alone. Since the electronic transitions are very energetic, power balances of helium-hydrogen plasmas compared to control krypton plasmas were measured previously [26, 38] using water bath calorimetry to determine whether this reaction has sufficient kinetics to merit its consideration as a practical power source. Excess power was absolutely measured from the helium-hydrogen plasma. For an input of 41.9 W, the total plasma power of the helium-hydrogen plasma measured by water bath calorimetry was 62.1 W corresponding to 20.2 W of excess power in 3 cm³ plasma volume. The excess power density and energy balance were high, 6.7 W/cm³ and -5.4×10^4 kJ/mole H_2 (280 eV/H atom), respectively.

B. Experiments to Test the Theoretical Predictions

The present paper tests theoretical predictions [1-5, 8-13, 38] that atomic and molecular hydrogen form stable states of lower energy than traditionally thought possible. Substantial spectroscopic differences are anticipated. For example, novel EUV atomic, molecular ion, and molecular spectral emission lines from transitions corresponding to energy levels given by Eqs. (2a) and (2c), Eq. (4), and Eq. (5), respectively, are predicted. The atomic and molecular ion lines have been shown previously [1-4, 26, 38] as well as a series of unique EUV lines assigned to $H_2(1/2)$ [4]. To test additional predictions, EUV spectroscopy was performed to search for emission that was characteristic of and identified $H_2(1/4)$. The rotational energies provide a very precise measure of I and the internuclear distance using well established theory [32]. Molecular emission was anticipated for high pressure argon-hydrogen plasmas excited by a 15 keV electron beam. Rotational lines for $H_2(1/4)$ were anticipated and sought in the 150-185 nm region. The spectral lines were compared to those predicted by Eqs. (15-16) corresponding to the internuclear distance of 1/4 that of H_2 given by Eq. (18). The predicted energies for the $v = 1 \rightarrow v = 0$ vibration-rotational series of $H_2(1/4)$ (Eqs. (15-16)) are

$$\begin{aligned} E_{vib-rot} &= p^2 E_{vib H_2(v=0 \rightarrow v=1)} \pm p^2 (J+1) E_{rot H_2} \\ &= 4^2 E_{vib H_2(v=0 \rightarrow v=1)} \pm 4^2 (J+1) E_{rot H_2}, \quad J = 0, 1, 2, 3, \dots \\ &= 8.254432 \text{ eV} \pm (J+1) 0.24144 \text{ eV} \end{aligned} \quad (22)$$

for $p = 4$. The assignment of the lines given by Eq. (22) to $H_2(1/4)$ is made essentially

absolute with the further match of the data with the predicted vibration-rotational spectrum with deuterium substitution and the match with the selection rules of $D_2(1/4)$ as well as $H_2(1/4)$.

The vibration-rotational transitions of $H_2(1/4)$ are allowed with nuclear spin-rotational coupling. The nuclear spin quantum number for the proton is $I = 1/2$, and the selection rule for nuclear spin transitions are $\Delta I = \pm 1$. These transition can couple to the rotational quantum states such that the P-branch transitions with $\Delta J = 1$ are allowed since the nuclear-rotational interaction is of the form $-\hbar C \mathbf{I}_k \cdot \mathbf{J}$ [39-41] where \mathbf{I}_k is the spin of the nucleus k , \mathbf{J} is the rotational angular momentum, C is the spin-rotational constant, and $\Delta I = 1$ to conserve angular momentum that is quantized in terms of units of \hbar . In addition, the transition corresponding to R(0) is allowed since the corresponding final state does not rotate and has a relative infinite half-life. Thus, the vibrational rotational spectrum of $H_2(1/4)$ is predicted to comprise only the R(0) line and the P branch.

For deuterium, the nuclear spin quantum number is $I = 1$, and the possible nuclear-spin transitions correspond to $\Delta I = \pm 1, 2$. The P-branch transitions are allowed as given before for $I = 1/2$. In the case that the rotational-state lifetime is very short (< 1 ps), radiative rotational transitions coupling to the nuclear spin are restricted to those having an initial $J = 0$ state with a relative infinite half-life, and the selection rules are determined by the nuclear hyperfine level transitions. Thus, to conserve angular momentum, the vibration-rotational spectrum of $D_2(1/4)$ is predicted to comprise peaks due to the transitions $J = 0$ to $J = 1$ and $J = 0$ to $J = 2$ corresponding to $\Delta I = 1$ and $\Delta I = 2$, respectively.

The experiment rotational energy for the $J = 0$ to $J = 1$ transition of D_2 is [35]

$$\Delta E = 0.00755 \text{ eV} \quad (23)$$

From, Eq. (16), the rotational energies of $D_2(1/4)$ with $p = 4$ are 16 times those of D_2 . Using Eqs. (13), (16), (18), and (23), the rotational energy absorbed by $D_2(1/4)$ with the transition from the state with the rotational quantum number J to one with the rotational quantum number J' is

$$\begin{aligned} \Delta E = E_{J'} - E_J &= \frac{p^2}{2} (0.00755) [J'(J'+1) - J(J+1)] \\ &= \frac{4^2}{2} (0.00755) [J'(J'+1) - J(J+1)] \\ &= 0.0604 [J'(J'+1) - J(J+1)] \text{ eV} \end{aligned} \quad (24)$$

For $J = 0$ to $J' = 1$, Eq. (24) gives the rotational energy as

$$\Delta E = 0.0604[2 - 0] \text{ eV} = 0.1208 \text{ eV} \quad (25)$$

and for $J = 0$ to $J' = 2$, Eq. (24) gives the rotational energy as

$$\Delta E = 0.0604[6 - 0] \text{ eV} = 0.3624 \text{ eV} \quad (26)$$

Similarly, as given in Ref [9], the vibration energies of $D_2(1/4)$ are $p^2 = 4^2 = 16$ times those of D_2 . Both the calculated and experimental vibrational energies, E_{vib} , for the D_2 $v = 1 \rightarrow v = 0$

transition [9, 32, 33] are

$$E_{vib} = 0.3709 \text{ eV} \quad (27)$$

and the vibrational energy for the $\nu = 1 \rightarrow \nu = 0$ transition of $D_2(1/4)$ [9] is

$$E_{vib} = p^2 0.3709 \text{ eV} = 4^2 0.3709 \text{ eV} = 5.9344 \text{ eV} \quad (28)$$

Thus, the vibration-rotational spectrum of $D_2(1/4)$ is predicted to comprise only two lines of energies that are equivalent to those of conventional P(1) and P(3) peaks [32] due to the transitions $J = 0$ to $J = 1$ and $J = 0$ to $J = 2$, respectively. The energies given by Eqs. (28) and (25-26) are

$$E_{vib/rot(P(1))} = (5.9344 - 0.1208) \text{ eV} = 5.8136 \text{ eV} \quad (29)$$

and

$$E_{vib/rot(P(3))} = (5.9344 - 0.3624) \text{ eV} = 5.5720 \text{ eV} \quad (30)$$

With the lifetime on the order of the reciprocal of the rotational frequency, the emission may be shifted by the Doppler energy. As shown in the Resonant Line Shape and Lamb Shift section of Ref. [8], the spectroscopic linewidth arises from the classical rise-time band-width relationship, and the Lamb Shift is due to conservation of energy and linear momentum and arises from the radiation reaction force between the electron and the photon. The radiation reaction force in the case of the vibration of the molecule corresponds to a Doppler energy, E_D , that is dependent on the motion of the electrons due to vibration. The Doppler energy of the electron is given by Eqs. (2.72) and (12.186) of Ref. [8], Eq. (196) of Ref. [9], and in Refs. [42-43]:

$$\bar{E}_D \approx 2\sqrt{E_K E_R} = E_{hv} \sqrt{\frac{2\bar{E}_K}{Mc^2}} \quad (31)$$

where E_R is the recoil energy which arises from the photon's linear momentum given by Eq. (2.67) of Ref. [8], E_K is the vibrational energy given by Eqs. (174-191) and (265-270) of Ref. [9], and M is the mass of the electron m_e . Substitution of Eq. (28) for E_K and Eqs (29) and (30) for E_{hv} of the P(1) and P(3) transitions, respectively, gives

$$\bar{E}_{D(P(1))} = E_{hv} \sqrt{\frac{2\bar{E}_K}{m_e c^2}} = 5.8136 \text{ eV} \sqrt{\frac{2e(5.9344 \text{ eV})}{m_e c^2}} = 0.02802 \text{ eV} \quad (32)$$

and

$$\bar{E}_{D(P(3))} = E_{hv} \sqrt{\frac{2\bar{E}_K}{m_e c^2}} = 5.5720 \text{ eV} \sqrt{\frac{2e(5.9344 \text{ eV})}{m_e c^2}} = 0.02685 \text{ eV} \quad (33)$$

In the case of the P(1) emission, the vibration-rotational energy is decreased by three times the Doppler energy given by Eq. (32) corresponding to the three thermodynamic degrees of freedom [44]; whereas, in the case of the P(3) emission, the vibration-rotational energy is decreased by the Doppler energy given by Eq. (33) corresponding to one thermodynamic degree of freedom. The one degree of freedom is due to coupling of the rotational energy to the vibrational energy in order to conserve angular momentum with $\Delta J = 2$ wherein the vibration only has one degree of

freedom.

The Doppler-shifted energies of the P(1) and P(3) peaks given by Eqs. (29-33) are

$$E_{vb/rot}(P(1)) = 5.8136 \text{ eV} - 3(0.02802 \text{ eV}) = 5.72954 \text{ eV} (216.40 \text{ nm}) \quad (34)$$

and

$$E_{vb/rot}(P3) = 5.5720 \text{ eV} - 0.02685 \text{ eV} = 5.5452 \text{ eV} (223.59 \text{ nm}) \quad (35)$$

The peaks are predicted to be Gaussian with a Doppler broadened half-width given by the Doppler energies of Eqs. (32) and (33). Furthermore, the relative intensity of the 216.40 nm peak compared to 223.59 nm peak is predicted to be 2:1 based on the degeneracy of $\Delta I=1$ corresponding to $I=-1$ to $I=0$ and $I=0$ to $I=1$; whereas, for $\Delta I=2$, only the $I=-1$ to $I=1$ transition is possible.

Ne^+ serves as a catalyst to form $H(1/2)$. In the latter case, the catalysis of $H(1)$ to $H(1/2)$ releases 40.8 eV, and the second ionization energy of neon is 40.96328 eV [31]. Ne^+ may absorb about 40.8 eV and ionize to Ne^{2+} which is resonant with the difference in energy between the $p=2$ and the $p=1$ states of atomic hydrogen given by Eqs. (2a) and (2c). Thus, Ne^+ may serve as a catalyst to cause the transition between these hydrogen states. In addition, the first neon excimer continuum Ne_2^* may also provide a net enthalpy that is a multiple of that of the potential energy of the hydrogen atom. The first ionization energy of neon is 21.56454 eV [31], and the first neon excimer continuum Ne_2^* has an excited state energy in the region of 15.92 eV [45]. The combination of reactions of Ne_2^* to $2Ne^+$, then, has a net enthalpy of reaction of 27.21 eV; thus, it may serve as a catalyst to form $H(1/2)$. The product of the catalysis reaction, $H(1/2)$, may further serve as both a catalyst and a reactant to form $H(1/4)$ [2-3].

In addition, the first ionization energy of Ar is 15.75962 eV [31]. The role of oxygen in the formation of the catalyst Ar^+ by ionization was discussed previously [38]. Since the first neon excimer continuum Ne_2^* has an excited state energy in the region of 15.92 eV [45], Ne_2^* can ionize Ar and Ar_2^* to the catalyst Ar^+ by an effect resonant energy transfer observed previously [46]. To enhance the reaction kinetics of Ar^+ catalyst, neon was added when deuterium replaced hydrogen in high pressure argon-hydrogen plasmas excited by a 15 keV electron beam where molecular vibration-rotational lines were sought to compare to theoretical predictions.

II. Experimental

Vibration-rotational emission of $H_2(1/4)$ and $D_2(1/4)$ was investigated using an electron gun provided by Rutgers University and described previously [46-47]. The gun initiated argon plasmas with 0.5-1% hydrogen and deuterium in the pressure range of 100-800 Torr wherein

0.5-1% neon was added to the argon-deuterium mixed plasmas to improve the deuterium substitution results. Using each ultrapure gas alone or mixture, the plasma cell was flushed, then pumped down, flushed again, and filled. Krypton replaced argon in the controls, and argon, neon, hydrogen, deuterium, nitrogen, oxygen, nitrogen-oxygen (50/50%), ammonia, carbon dioxide, water vapor, 0.5-1% hydrogen or deuterium mixed plasmas, and argon or krypton with oxygen addition up to 100% oxygen served as further controls.

The electrons were accelerated with a high voltage of 12.5 keV at a beam current of $10 \mu\text{A}$. The electron gun was sealed with a thin (300 nm thickness) SiN_x foil that served as a 1 mm^2 electron window to the cell at high gas pressure (760 Torr). The beam energy was deposited by hitting the target gases, and the light emitted by beam excitation exited the cell through a MgF_2 window mounted at the entrance of a normal incidence McPherson 0.2 meter monochromator (Model 302) equipped with a 1200 lines/mm holographic grating with a platinum coating. The wavelength region covered by the monochromator was 5 – 560 nm. The EUV spectrum was recorded with a photomultiplier tube (PMT). The wavelength resolution was about 0.7 nm (FWHM) with an entrance and exit slit width of 200 μm . The increment was 0.1 nm and the dwell time was 1 s. The PMT (Model R8486, Hamamatsu) used has a spectral response in the range of 115-320 nm with a peak efficiency at about 225 nm. The emission was essentially flat for $200 < \lambda > 275 \text{ nm}$, but a notch in the response of about 20% existed in the short wavelength range with a minimum at 150 nm. Peak assignments were determined by an external calibration against standard line emissions.

III. Results and Discussion

A. Detection of Fractional Rydberg State Molecular Hydrogen $\text{H}_2(1/4)$

The 100-350 nm spectrum of a 783 Torr plasma of krypton containing about 1% hydrogen is shown in Figure 1. Only the excimer continua of krypton were observed as reported by Ulrich, Wieser, and Murnick [47].

The observation of emission due to the reaction $\text{H}(1/4) + \text{H}^+ \rightarrow \text{H}_2(1/4)^+$ at low pressure (< 1 Torr) reported previously [38] indicates that $\text{H}(1/4)$ formed in the argon-hydrogen plasma. Molecular formation was anticipated under high-pressure conditions (~ 760 Torr). Thus, EUV spectroscopy of argon-hydrogen plasmas was performed to search for $\text{H}_2(1/4)$ from $\text{H}(1/4)$ formed by Ar^+ as a catalyst. The normal incidence spectrometer was used at high pressure which required a window and an electron beam to maintain a plasma. Since the 15 keV beam rapidly transfers energy to the target gas and produces a large population of species with energies of a few 10's of eVs of kinetic energy, it was anticipated that the beam could directly or

indirectly collisionally excite vibration-rotational states of $H_2(1/4)$. The corresponding emission provides a direct measure of the internuclear distance; thus, this method provides the possibility of direct confirmation of $H_2(1/4)$.

The atmospheric-pressure argon plasma formed with the 15 keV electron beam forms Ar^+ which serves as a catalyst when H is present to form states given by Eqs. (2a) and (2c). Thus, spectra were recorded on argon-hydrogen plasmas maintained with a 15 keV electron beam. The 100-350 nm spectrum of a 450 Torr plasma of argon containing about 1% hydrogen is shown in Figure 2. Lyman α was observed at 121.6 nm with an adjoining H_2 band, the third continuum of Ar was observed at 200 nm, O I was observed at 130.7 nm, and the $OH(A-X)$ band was observed at 309.7 nm. A series of sharp, evenly-spaced lines was observed in the region 145-185 nm. The only possibilities for peaks of the instrument width are those due to rotation or electronic emission from atoms or ions. The series was not observed when krypton replaced argon. Additional controls of hydrogen, oxygen, nitrogen, nitrogen-oxygen (50/50%), ammonia, carbon dioxide, water vapor, and these plasmas mixed with hydrogen were also negative for the series. No hydrogen lines and no strong O I or O II lines matches any of the lines [33]. In the case that O II is a possibility for some of the lines, other O II lines of equal oscillator strength were not observed. The O I line at 130.6029 nm having an oscillator strength of over 100 times that of O II lines in this region [33] was weak which made the assignment to O II lines unlikely. Furthermore, no combination of O species exclusively matches the evenly spaced lines in this region. The lines were not observed with argon or krypton with oxygen addition up to 50%, and the lines, when observed with argon, 1% hydrogen, and trace oxygen, did not increase in intensity upon addition of additional oxygen. The series was not observed with argon alone, and only Ar VII and Ar VIII are possible in this region which is not possible at this pressure. Furthermore, no argon species match the observed lines [33].

The series matched the P branch of $H_2(1/4)$ for the vibrational transition $v = 1 \rightarrow v = 0$. P(1), P(2), P(3), P(4), P(5), and P(6) were observed at 155.0 nm, 160.2 nm, 165.8 nm, 171.1 nm, 178.0 nm, and 183.2 nm, respectively. The sharp peak at 147.3 nm may be the first member of the R branch, R(0). Other than R(0), R-branch lines appeared to correspond to forbidden transitions in agreement with predictions given in Sec. IB. The plot of the energies of the peaks shown in Figure 2 is shown in Figure 3. The slope of the linear curve fit is 0.241 eV with an intercept of 8.21 eV which matches Eq. (22) very well for $p = 4$. The series matches the predicted $v = 1 \rightarrow v = 0$ vibrational energy of $H_2(1/4)$ of 8.25 eV (Eq. (15)) and its predicted rotational energy spacing of 0.241 eV (Eq. (16)) with $\Delta J = +1; J = 1, 2, 3, 4, 5, 6$ and $\Delta J = -1; J = 0$ where J is the rotational quantum number of the final state.

Using Eqs. (16) and (18) with the measured rotational energy spacing of 0.241 eV establishes an internuclear distance of 1/4 that of the ordinary hydrogen species for $H_2(1/4)$.

This technique which is the best measure of the bond distance of any diatomic molecule identifies and unequivocally confirms $H_2(1/4)$.

A possible confirmation of the lines identified in this study has been published previously. Ulrich, Wieser, and Murnick [47] compared the third continuum of argon gas with a very pure gas and a spectrum in which the gas was slightly contaminated by oxygen as evidenced by the second order of the 130 nm resonance lines at 260 nm. A series of very narrow lines at the instrument width were observed in the 145-185 nm region. These lines shown in Figure 6 of Ref. [47] matched those in Figure 2. The lines having an intensity profile that was characteristic of that of a P-branch are plotted in Figure 4. The slope of the linear curve fit is 0.24 eV with an intercept of 8.24 eV which matches Eq. (22) very well for $p = 4$. The series matches the predicted $\nu = 1 \rightarrow \nu = 0$ vibrational energy of $H_2(1/4)$ of 8.25 eV (Eq. (15)) and its predicted rotational energy spacing of 0.24 eV (Eq. (16)) with $\Delta J = +1; J = 1, 2, 3, 4, 5, 6$ and $\Delta J = -1; J = 0$ where J is the rotational quantum number of the final state. With this assignment, all of the peaks in Figure 6 of Ref. [47] could be identified; whereas, the evenly-spaced lines could not be unambiguously assigned by Ulrich et al [47]. The series was not observed in krypton and xenon plasmas. The determination of the presence of the common contaminant, hydrogen, in the argon plasmas is warranted in future studies.

B. Detection of Fractional Rydberg State Molecular Hydrogen $D_2(1/4)$

The assignment of the lines given by Eq. (22) to $H_2(1/4)$ is made essentially absolute with the further match of the data with the predicted vibration-rotational spectrum with deuterium substitution and the match with the selection rules of $D_2(1/4)$ as well as $H_2(1/4)$ given in Sec. IB. The 100-350 nm spectrum of a 783 Torr plasma of argon containing about 0.5-1% neon, 0.5% hydrogen, and 0.5% deuterium is shown in both Figures 5 and 6. The effect of the addition of neon to form the catalyst Ar^+ was evidenced by a decrease in intensity of the third continuum of argon and a shift of its emission from 210 nm to 190 nm as observed previously in the case of the addition of oxygen [38, 47]. In Figure 5, Lyman α was observed at 121.6 nm with an adjoining D_2 band, the third continuum of Ar was observed at 210 nm, and an $OH(A-X)/OD(A-X)$ band was observed at 308.9 nm. A series of sharp, evenly-spaced lines was observed in the region 145-185 nm, and the second order peaks were observed in the 310-350 nm region. The series matched the P branch of $H_2(1/4)$ for the vibrational transition $\nu = 1 \rightarrow \nu = 0$ given by Eq. (22). P(1), P(2), P(3), P(4), P(5), and P(6) were observed at 154.2 nm, 159.9 nm, 165.5 nm, 171.9 nm, 177.7 nm, and 183.2 nm, respectively. The peak at 147 nm may be the first member of the R branch, R(0). The slope of a linear curve fit is 0.246 eV with an intercept of 8.23 eV which matches Eq. (22) very well for $p = 4$.

In addition, two broad peaks of relative intensity 2:1 were observed at 216.4 and 223.6 nm. The peaks closely matched the Doppler shifted and broadened emission of $D_2(1/4)$ for the vibrational transition $\nu = 1 \rightarrow \nu = 0$ and rotational energies of P(1) and P(3) given by Eqs. (34) and (35), respectively.

The 100-350 nm spectrum of a 783 Torr plasma of argon containing about 0.5-1% neon and 1% deuterium is shown in Figures 7 and 8. An intense D_2 band was observed in the 150-185 nm region that replaced the P branch of $H_2(1/4)$ observed in Figures 2, 5, and 6. The two broad peaks of relative intensity 2:1 were observed at 216.4 and 223.6 nm. The peaks matched the Doppler shifted and broadened emission of $D_2(1/4)$ for the vibrational transition $\nu = 1 \rightarrow \nu = 0$ and rotational energies of P(1) and P(3) given by Eqs. (34) and (35) respectively. The intensity of the $D_2(1/4)$ peaks increased in intensity relative to those shown in Figures 5 and 6 with the increase in deuterium concentration.

Due to the board width of each peak, the only possible known assignment of each of the two peaks is a molecular band comprising a series of unresolved vibration-rotational lines. However, no molecule was found that matched these wavelengths, and no known molecule only emits two bands alone. Air contaminants and other possible molecules were eliminated. Plasmas of krypton, argon, neon, hydrogen, deuterium, nitrogen, oxygen, nitrogen-oxygen (50/50%), ammonia, carbon dioxide, water vapor, and 0.5-1% hydrogen or deuterium mixed plasmas showed no lines that matched the 216.4 and 223.6 nm peaks.

The second order peaks which allow for a determination of the peak profile at twice the resolution are shown in Figure 9. In each case, the data matched a Gaussian profile having the X^2 and R^2 values given in Figure 9. The full-width-half-maximum (FWHM) of each Gaussian curve, $\Delta\lambda_G$, was about 1.67 and 1.10 nm, respectively. $\Delta\lambda_G$ of each Gaussian results from the Doppler ($\Delta\lambda_D$) and instrumental ($\Delta\lambda_I$) half-widths:

$$\Delta\lambda_G = \sqrt{\Delta\lambda_D^2 + \Delta\lambda_I^2} \quad (36)$$

The instrument half-width, $\Delta\lambda_I$, in our experiments was 0.66 nm. Thus, $\Delta\lambda_D$ for the 216.4 and 223.6 nm peaks was 1.53 and 0.88 nm, respectively. The corresponding energy widths are 0.04 and 0.022 eV in agreement with that predicted by Eqs. (32) and (33). The relative peak intensities were about 2:1 also in agreement with predictions given in Sec. IB. The Gaussian profile eliminates the possibility to assign the peaks to molecular bands. The elimination of known explanations indicate a new result. Since the novel peaks were only observed with argon and hydrogen or deuterium present, new hydrogen, argon, or argon-hydrogen species are possibilities. Based on the peak energies, shape, and intensities with no match to known molecules including N_2 , N_2^+ , NO , NO_2 , NH_3 , O_2 , and H_2O , the deuterium spectra and the results given in Sec. IIIA dispositively identified the emitting species in the 145-185 and 215-

225 nm ranges as $H_2(1/4)$ and $D_2(1/4)$, respectively.

IV. Conclusion

In this study we made specific theoretical predictions regarding the $H_2(1/4)$ and $D_2(1/4)$ vibration-rotational spectra and tested them with standard, easily interpretable experiments. The results show that these new states of hydrogen are formed in a catalytic plasma reaction.

The atomic states $H(1/p)$ were identified previously [1-4] by the spectroscopic observation of emission lines occurring at energies that are an extension of the Rydberg series to lower states, and a corresponding molecular ion $H_2(1/4)^+$ was identified by vibrational-rotational series that established an internuclear distance of 1/4 that of the ordinary hydrogen species. It was also previously reported that the molecular hydrogen gas product was isolated by liquefaction at liquid nitrogen temperature and by decomposition of compounds previously found to contain the corresponding hydride ions $H^-(1/p)$ [9, 20, 28-30]. Singlet peaks upfield of H_2 with a predicted integer spacing of 0.64 ppm at 3.47, 3.02, 2.18, 1.25, 0.85, and 0.22 ppm identified as the consecutive series $H_2(1/2)$, $H_2(1/3)$, $H_2(1/4)$, $H_2(1/5)$, $H_2(1/6)$, and $H_2(1/7)$ and $H_2(1/10)$ at -1.8 ppm provides powerful confirmation of the existence of $H_2(1/p)$ [38]. Furthermore, the 1H NMR spectra of gases from the thermal decomposition of KH^+I matched those of LN-condensable hydrogen which provides strong support that compounds such as KH^+I contain hydride ions $H^-(1/p)$ in the same fractional quantum state p as the observed $H_2(1/p)$ [38]. Observational agreement with predicted positions of upfield-shifted 1H MAS NMR peaks of the compounds [9, 20, 28-30, 38], catalyst reactions [18, 22-23], very high (>100 eV) H energies [14-16], substantial excess thermal energy [4, 20, 26, 38], and spectroscopic data supports this conclusion [1-5, 18, 20].

The gold standard spectroscopic study to identify and characterize a diatomic molecule is vibration-rotational spectroscopy with isotope substitution. As shown in Figure 2, a series of sharp, evenly-spaced lines was observed from an atmospheric-pressure argon-hydrogen plasma maintained with a 15 keV electron gun. The series matched R(0) and the P branch of $H_2(1/4)$ for the vibrational transition $\nu = 1 \rightarrow \nu = 0$. The slope of the linear curve fit was 0.241 eV with an intercept of 8.21 eV which matches Eq. (22) very well for $p = 4$. The series matched the predicted $\nu = 1 \rightarrow \nu = 0$ vibrational energy of $H_2(1/4)$ of 8.25 eV (Eq. (15)) and its predicted rotational energy spacing of 0.241 eV (Eq. (16)) with $\Delta J = +1; J = 1, 2, 3, 4, 5, 6$ and $\Delta J = -1; J = 0$ where J is the rotational quantum number of the final state. Using Eqs. (16) and (18), the unprecedented energy spacing of 4^2 times that of hydrogen established the internuclear distance as 1/4 that of H_2 and identified $H_2(1/4)$.

With deuterium substitution, two broad peaks of relative intensity 2:1 were observed at 216.4 and 223.6 nm. The peaks matched the Doppler shifted and broadened emission of $D_2(1/4)$ for the vibrational transition $v=1 \rightarrow v=0$ and rotational energies of P(1) and P(3) given by Eqs. (34) and (35), respectively. In each case, the second-order peaks matched a Gaussian profile with a Doppler half-width of 1.53 and 0.88 nm, respectively, corresponding to 0.04 and 0.02 eV in agreement with that predicted by Eqs. (32) and (33). The relative peak intensities were about 2:1 also in agreement with predictions. The deuterium substitution results unequivocally identified $D_2(1/4)$, a deuterium molecule with an internuclear distance of 1/4 that of ordinary D_2 .

The observation of the predicted vibration-rotation spectra for both isotopes provides substantial evidence for the existence of new states of hydrogen formed by a catalytic plasma reaction. The existence of excited vibration-rotational levels of $H_2(1/p)$ and $D_2(1/p)$ presents the possibility of a laser using a transition from a vibration-rotational level to another lower-energy-level other than one with a significant Boltzmann population at the cell neutral-gas temperature (e.g. one with both v and $J=0$). A laser may be realized using cavities and mirrors that are appropriate for the desired wavelength similar to those of current lasers based on molecular vibration-rotational levels such as the CO_2 laser. However, an advantage exists to produce laser light at much shorter wavelengths. The current results anticipate lasers based on vibration-rotational levels of $H_2(1/4)$ and $D_2(1/4)$ that lase over the regions visible to soft X-ray. Such lasers have significant applications in photolithography at ultraviolet (UV) and EUV wavelengths.

Acknowledgments

Special thanks to D. E. Murnick and M. Salvermoser of Rutgers University for providing the 15 keV electron gun.

References

1. R. L. Mills, P. Ray, "Extreme Ultraviolet Spectroscopy of Helium-Hydrogen Plasma," *J. Phys. D, Applied Physics*, Vol. 36, (2003), pp. 1535-1542.
2. R. L. Mills, P. Ray, B. Dhandapani, M. Nansteel, X. Chen, J. He, "New Power Source from Fractional Quantum Energy Levels of Atomic Hydrogen that Surpasses Internal Combustion," *J Mol. Struct.*, Vol. 643, No. 1-3, (2002), pp. 43-54.
3. R. Mills, P. Ray, "Spectral Emission of Fractional Quantum Energy Levels of Atomic Hydrogen from a Helium-Hydrogen Plasma and the Implications for Dark Matter," *Int. J.*

- Hydrogen Energy, Vol. 27, No. 3, pp. 301-322.
- 4. R. L. Mills, P. Ray, J. Dong, M. Nansteel, B. Dhandapani, J. He, "Spectral Emission of Fractional-Principal-Quantum-Energy-Level Atomic and Molecular Hydrogen," Vibrational Spectroscopy, Vol. 31, No. 2, (2003), pp. 195-213.
 - 5. R. Mills, P. Ray, "Vibrational Spectral Emission of Fractional-Principal-Quantum-Energy-Level Hydrogen Molecular Ion," Int. J. Hydrogen Energy, Vol. 27, No. 5, (2002), pp. 533-564.
 - 6. N. V. Sidgwick, *The Chemical Elements and Their Compounds*, Volume I, Oxford, Clarendon Press, (1950), p.17.
 - 7. M. D. Lamb, *Luminescence Spectroscopy*, Academic Press, London, (1978), p. 68.
 - 8. R. Mills, *The Grand Unified Theory of Classical Quantum Mechanics*, September 2001 Edition, BlackLight Power, Inc., Cranbury, New Jersey, Distributed by Amazon.com; January (2004) Edition posted at www.blacklightpower.com.
 - 9. R. L. Mills, "The Nature of the Chemical Bond Revisited and an Alternative Maxwellian Approach," submitted. Posted at <http://www.blacklightpower.com/pdf/technical/H2PaperTableFiguresCaptions111303.pdf>.
 - 10. R. Mills, J. Dong, Y. Lu, "Observation of Extreme Ultraviolet Hydrogen Emission from Incandescently Heated Hydrogen Gas with Certain Catalysts," Int. J. Hydrogen Energy, Vol. 25, (2000), pp. 919-943.
 - 11. R. Mills and M. Nansteel, P. Ray, "Argon-Hydrogen-Strontium Discharge Light Source," IEEE Transactions on Plasma Science, Vol. 30, No. 2, (2002), pp. 639-653.
 - 12. R. Mills and M. Nansteel, P. Ray, "Bright Hydrogen-Light Source due to a Resonant Energy Transfer with Strontium and Argon Ions," New Journal of Physics, Vol. 4, (2002), pp. 70.1-70.28.
 - 13. R. Mills, M. Nansteel, and P. Ray, "Excessively Bright Hydrogen-Strontium Plasma Light Source Due to Energy Resonance of Strontium with Hydrogen," J. of Plasma Physics, Vol. 69, (2003), pp. 131-158.
 - 14. R. L. Mills, P. Ray, B. Dhandapani, R. M. Mayo, J. He, "Comparison of Excessive Balmer α Line Broadening of Glow Discharge and Microwave Hydrogen Plasmas with Certain Catalysts," J. of Applied Physics, Vol. 92, No. 12, (2002), pp. 7008-7022.
 - 15. R. L. Mills, P. Ray, B. Dhandapani, J. He, "Comparison of Excessive Balmer α Line Broadening of Inductively and Capacitively Coupled RF, Microwave, and Glow Discharge Hydrogen Plasmas with Certain Catalysts," IEEE Transactions on Plasma Science, Vol. 31, No. (2003), pp. 338-355.
 - 16. R. L. Mills, P. Ray, "Substantial Changes in the Characteristics of a Microwave Plasma Due to Combining Argon and Hydrogen," New Journal of Physics, www.njp.org, Vol. 4, (2002),

pp. 22.1-22.17.

17. J. Phillips, C. Chen, "Evidence of Energetic Reaction Between Helium and Hydrogen Species in RF Generated Plasmas," submitted.
18. R. L. Mills, P. Ray, "A Comprehensive Study of Spectra of the Bound-Free Hyperfine Levels of Novel Hydride Ion H^- (1/2), Hydrogen, Nitrogen, and Air," Int. J. Hydrogen Energy, Vol. 28, No. 8, (2003), pp. 825-871.
19. R. Mills, "Spectroscopic Identification of a Novel Catalytic Reaction of Atomic Hydrogen and the Hydride Ion Product," Int. J. Hydrogen Energy, Vol. 26, No. 10, (2001), pp. 1041-1058.
20. R. Mills, P. Ray, B. Dhandapani, W. Good, P. Jansson, M. Nansteel, J. He, A. Voigt, "Spectroscopic and NMR Identification of Novel Hydride Ions in Fractional Quantum Energy States Formed by an Exothermic Reaction of Atomic Hydrogen with Certain Catalysts," submitted.
21. H. Conrads, R. Mills, Th. Wrubel, "Emission in the Deep Vacuum Ultraviolet from a Plasma Formed by Incandescently Heating Hydrogen Gas with Trace Amounts of Potassium Carbonate," Plasma Sources Science and Technology, Vol. 12, (2003), pp. 389-395.
22. R. Mills, P. Ray, R. M. Mayo, "CW HI Laser Based on a Stationary Inverted Lyman Population Formed from Incandescently Heated Hydrogen Gas with Certain Group I Catalysts," IEEE Transactions on Plasma Science, Vol. 31, No. 2, (2003), pp. 236-247.
23. R. L. Mills, P. Ray, "Stationary Inverted Lyman Population Formed from Incandescently Heated Hydrogen Gas with Certain Catalysts," J. Phys. D, Applied Physics, Vol. 36, (2003), pp. 1504-1509.
24. R. Mills, P. Ray, R. M. Mayo, "The Potential for a Hydrogen Water-Plasma Laser," Applied Physics Letters, Vol. 82, No. 11, (2003), pp. 1679-1681.
25. R. L. Mills, P. C. Ray, R. M. Mayo, M. Nansteel, B. Dhandapani, J. Phillips, "Spectroscopic Study of Unique Line Broadening and Inversion in Low Pressure Microwave Generated Water Plasmas," submitted.
26. R. L. Mills, X. Chen, P. Ray, J. He, B. Dhandapani, "Plasma Power Source Based on a Catalytic Reaction of Atomic Hydrogen Measured by Water Bath Calorimetry," Thermochimica Acta, Vol. 406/1-2, pp. 35-53.
27. R. Mills, B. Dhandapani, M. Nansteel, J. He, P. Ray, "Liquid-Nitrogen-Condensable Molecular Hydrogen Gas Isolated from a Catalytic Plasma Reaction," submitted.
28. R. Mills, B. Dhandapani, M. Nansteel, J. He, T. Shannon, A. Echezuria, "Synthesis and Characterization of Novel Hydride Compounds," Int. J. of Hydrogen Energy, Vol. 26, No. 4, (2001), pp. 339-367.
29. R. Mills, B. Dhandapani, N. Greenig, J. He, "Synthesis and Characterization of Potassium

- Iodo Hydride," Int. J. of Hydrogen Energy, Vol. 25, Issue 12, December, (2000), pp. 1185-1203.
30. R. Mills, B. Dhandapani, M. Nansteel, J. He, A. Voigt, "Identification of Compounds Containing Novel Hydride Ions by Nuclear Magnetic Resonance Spectroscopy," Int. J. Hydrogen Energy, Vol. 26, No. 9, (2001), pp. 965-979.
31. D. R. Lide, *CRC Handbook of Chemistry and Physics*, 79 th Edition, CRC Press, Boca Raton, Florida, (1998-9), pp. 10-175-10.177.
32. M. Karplus, R. N. Porter, *Atoms and Molecules an Introduction for Students of Physical Chemistry*, The Benjamin/Cummings Publishing Company, Menlo Park, California, (1970), pp. 447-484.
33. NIST Atomic Spectra Database, www.physics.nist.gov/cgi-bin/AtData/display.ksh.
34. D. A. McQuarrie, *Quantum Chemistry*, University Science Books, Mill Valley, CA, (1983), pp. 206-237.
35. P. W. Atkins, *Physical Chemistry*, Second Edition, W. H. Freeman, San Francisco, (1982), p. 589.
36. H. Beutler, Z. Physical Chem., "Die dissoziationswarme des wasserstoffmolekuls H_2 , aus einem neuen ultravioletten resonanzbandenzug bestimmt," Vol. 27B, (1934), pp. 287-302.
37. G. Herzberg, L. L. Howe, "The Lyman bands of molecular hydrogen," Can. J. Phys., Vol. 37, (1959), pp. 636-659.
38. R. L. Mills, Y. Lu, J. He, M. Nansteel, P. Ray, X. Chen, A. Voigt, B. Dhandapani, "Spectral Identification of New States of Hydrogen," submitted.
39. W. T. Raynes, N. Panteli, "The extraction of a nuclear magnetic shielding function for the H_2 molecule from spin-rotation and isotope shift data," Molecular Physics, Vol. 48, No. 3, (1983), pp. 439-449.
40. D. Sundholm, J. Gauss, R. Ahlrichs, "The electron correlation contribution to the nuclear magnetic shielding tensor of the hydrogen molecule," Chemical Physics Letters, Vol. 243, (1995), pp. 264-268.
41. W. T. Raynes, N. Panteli, "The nuclear spin-spin coupling in the hydrogen molecule: Its equilibrium value and bond-length dependence," Chemical Physics Letters, Vol. 94, (1983), pp. 558-560.
42. T. C. Gibb, *Principles of Mössbauer Spectroscopy*, Chapman and Hall: London (1977), Chp. 1.
43. U. Gonser, From a Strange Effect to Mössbauer Spectroscopy in *Mössbauer Spectroscopy*, U. Gonser, Ed. Springer-Verlag: New York (1975), pp. 1-51.
44. A. Beiser, *Concepts of Modern Physics*, 4th Edition, McGraw-Hill Book Company, New York, (1978), pp. 312-354.

45. P. Kurunczi, H. Shah, and K. Becker, "Hydrogen Lyman- α and Lyman- β emissions from high-pressure microhollow cathode discharges in $Ne - H_2$ mixtures," *J. Phys. B: At. Mol. Opt. Phys.*, Vol. 32, (1999), L651-L658.
46. J. Wieser, D. E. Murnick, A. Ulrich, H. A Higgins, A. Liddle, W. L. Brown, "Vacuum ultraviolet rare gas excimer light source," *Rev. Sci. Instrum.*, Vol. 68, No. 3, (1997), pp. 1360-1364.
47. A. Ulrich, J. Wieser, D. E. Murnick, "Excimer Formation Using Low Energy Electron Beam Excitation," *Second International Conference on Atomic and Molecular Pulsed Lasers, Proceedings of SPIE*, Vol. 3403, (1998), pp. 300-307.

Table 1. The Maxwellian closed-form calculated and experimental parameters of H_2 , D_2 , H_2^+ and D_2^+ .

Parameter	Calculated	Experimental	Eqs. ^a
H_2 Bond Energy	4.478 eV	4.478 eV	261
D_2 Bond Energy	4.556 eV	4.556 eV	263
H_2^+ Bond Energy	2.654 eV	2.651 eV	230
D_2^+ Bond Energy	2.696 eV	2.691 eV	232
H_2 Total Energy	31.677 eV	31.675 eV	257
D_2 Total Energy	31.760 eV	31.760 eV	258
H_2 Ionization Energy	15.425 eV	15.426 eV	259
D_2 Ionization Energy	15.463 eV	15.466 eV	260
H_2^+ Ionization Energy	16.253 eV	16.250 eV	228
D_2^+ Ionization Energy	16.299 eV	16.294 eV	229
H_2^+ Magnetic Moment	$9.274 \times 10^{-24} JT^{-1}$	$9.274 \times 10^{-24} JT^{-1}$	328-334
	μ_B	μ_B	
Absolute H_2 Gas-Phase NMR Shift	-28.0 ppm	-28.0 ppm	345
H_2 Internuclear Distance ^b	0.748 Å $\sqrt{2}a_o$	0.741 Å	248
D_2 Internuclear Distance ^b	0.748 Å $\sqrt{2}a_o$	0.741 Å	248
H_2^+ Internuclear Distance ^c	1.058 Å $2a_o$	1.06 Å	217
D_2^+ Internuclear Distance ^b	1.058 Å $2a_o$	1.0559 Å	217
H_2 Vibrational Energy	0.517 eV	0.516 eV	269
D_2 Vibrational Energy	0.371 eV	0.371 eV	274
$H_2 \omega_e x_e$	$120.4 cm^{-1}$	$121.33 cm^{-1}$	271
$D_2 \omega_e x_e$	$60.93 cm^{-1}$	$61.82 cm^{-1}$	275
H_2^+ Vibrational Energy	0.270 eV	0.271 eV	238
D_2^+ Vibrational Energy	0.193 eV	0.196 eV	242
H_2 J=1 to J=0 Rotational Energy ^b	0.0148 eV	0.01509 eV	290
D_2 J=1 to J=0 Rotational Energy ^b	0.00741 eV	0.00755 eV	278-283, 290
H_2^+ J=1 to J=0 Rotational Energy ^c	0.00740 eV	0.00739 eV	286
D_2^+ J=1 to J=0 Rotational Energy ^b	0.00370 eV	0.003723 eV	278-286

^a Ref. [9].

^b The internuclear distances are not corrected for the reduction due to \bar{E}_{acc} .

^c The internuclear distances are not corrected for the increase due to \bar{E}_{acc} .

Figure Captions

Figure 1. The 100-350 nm spectrum of a 783 Torr plasma of krypton containing about 1% hydrogen. Only the excimer continua of krypton were observed.

Figure 2. The 100-350 nm spectrum of a 450 Torr plasma of argon containing about 1% hydrogen. Lyman α was observed at 121.6 nm with an adjoining H_2 band, the third continuum of Ar was observed at 200 nm, O I was observed at 130.7 nm, and the $OH(A - X)$ band was observed at 309.7 nm. A series of sharp, evenly-spaced lines was observed in the region 145-185 nm. The series matched the P branch of $H_2(1/4)$ for the vibrational transition $v=1 \rightarrow v=0$. P(1), P(2), P(3), P(4), P(5), and P(6) were observed at 155.0 nm, 160.2 nm, 165.8 nm, 171.1 nm, 178.0 nm, and 183.2 nm, respectively. The sharp peak at 147.3 nm may be the first member of the R branch, R(0). The R-branch lines appeared to correspond to forbidden transitions.

Figure 3. The plot of the energies of the peaks shown in Figure 2. The slope of the linear curve fit is 0.241 eV with an intercept of 8.21 eV which matches Eq. (22) very well for $p = 4$. The series matches the predicted $v=1 \rightarrow v=0$ vibrational energy of $H_2(1/4)$ of 8.25 eV (Eq. (15)) and its predicted rotational energy spacing of 0.241 eV (Eq. (16)) with $\Delta J = +1; J = 1, 2, 3, 4, 5, 6$ and $\Delta J = -1; J = 0$ where J is the rotational quantum number of the final state.

Figure 4. The plot of the energies of the lines shown in Figure 6 of Ref. [47]. The slope of the linear curve fit is 0.24 eV with an intercept of 8.24 eV which matches Eq. (22) very well for $p = 4$. The series matches the predicted $v=1 \rightarrow v=0$ vibrational energy of $H_2(1/4)$ of 8.25 eV (Eq. (15)) and its predicted rotational energy spacing of 0.24 eV (Eq. (16)) with $\Delta J = +1; J = 1, 2, 3, 4, 5, 6$ and $\Delta J = -1; J = 0$ where J is the rotational quantum number of the final state. The intensity profile of the lines corresponding to $\Delta J = +1$ matched that of a P-branch. The peak at 8.46 eV was weak.

Figure 5. The 100-350 nm spectrum of a 485 Torr plasma of argon containing about 0.5-1% neon, 0.5% hydrogen, and 0.5% deuterium. Lyman α was observed at 121.6 nm with an adjoining D_2 band, the third continuum of Ar was observed at 210 nm, and an $OH(A - X)/OD(A - X)$ band was observed 308.9 nm. A series of sharp, evenly-spaced lines was observed in the region 145-185 nm, and the second order peaks were observed in the 310-350 nm region. The series matched the P branch of $H_2(1/4)$ for the vibrational transition $v=1 \rightarrow v=0$ given by Eq. (22). P(1), P(2), P(3), P(4), P(5), and P(6) were observed at 154.21 nm, 159.91 nm, 165.51 nm, 171.91 nm, 177.71 nm, and 183.21 nm, respectively. The peak at 147 nm may be the first member of the R branch, R(0). The slope of a linear curve fit is 0.246 eV with an intercept of 8.23 eV which matches Eq. (22) very well for $p = 4$. In addition, two

broad peaks of relative intensity 2:1 were observed at 216.4 and 223.6 nm. The peaks matched the Doppler shifted and broadened emission of $D_2(1/4)$ for the vibrational transition $\nu = 1 \rightarrow \nu = 0$ and rotational energies of P(1) and P(3) given by Eqs. (34) and (35), respectively.

Figure 6. The 100-350 nm spectrum of a 750 Torr plasma of argon containing about 0.5-1% neon, 0.5% hydrogen, and 0.5% deuterium. These results with the results shown in Figure 5 demonstrates the reproducibility of the $H_2(1/4)$ and $D_2(1/4)$ vibration-rotational spectra.

Figure 7. The 100-350 nm spectrum of a 470 Torr plasma of argon containing about 0.5-1% neon and 1% deuterium. Lyman α was observed at 121.6 nm with an adjoining D_2 band. An intense D_2 band was observed in the 150-185 nm region that replaced the P branch of $H_2(1/4)$ observed in Figures 2, 5, and 6. The third continuum of Ar was observed at 210 nm, and the $OD(A - X)$ bands were observed at 282.7 and 308.6 nm. Two broad peaks of relative intensity 2:1 were observed at 216.4 and 223.6 nm. The peaks matched the Doppler shifted and broadened emission of $D_2(1/4)$ for the vibrational transition $\nu = 1 \rightarrow \nu = 0$ and rotational energies of P(1) and P(3) given by Eqs. (34) and (35) respectively. The intensity of the $D_2(1/4)$ peaks increased in intensity relative to those shown in Figures 5 and 6 with the increase in deuterium concentration.

Figure 8. The 100-325 nm spectrum of a 600 Torr plasma of argon containing about 0.5-1% neon and 1% deuterium. These results with the results shown in Figure 7 demonstrates the reproducibility of the $D_2(1/4)$ vibration-rotational spectrum.

Figure 9. The 425-455 nm spectrum of a 100 Torr plasma of argon containing about 0.5-1% neon and 1% deuterium. The second order of the 216.4 and 223.6 nm peaks were observed. In each case, the data matched a Gaussian profile having the X^2 and R^2 values indicated. The full-width-half-maximum (FWHM) of each Gaussian curve, $\Delta\lambda_G$, was about 1.67 and 1.10 nm corresponding to a Doppler half-width of 1.53 and 0.88 nm, respectively. The corresponding energy widths are 0.04 and 0.022 eV in agreement with that predicted by Eqs. (32) and (33). The relative peak intensities were about 2:1 also in agreement with predictions.

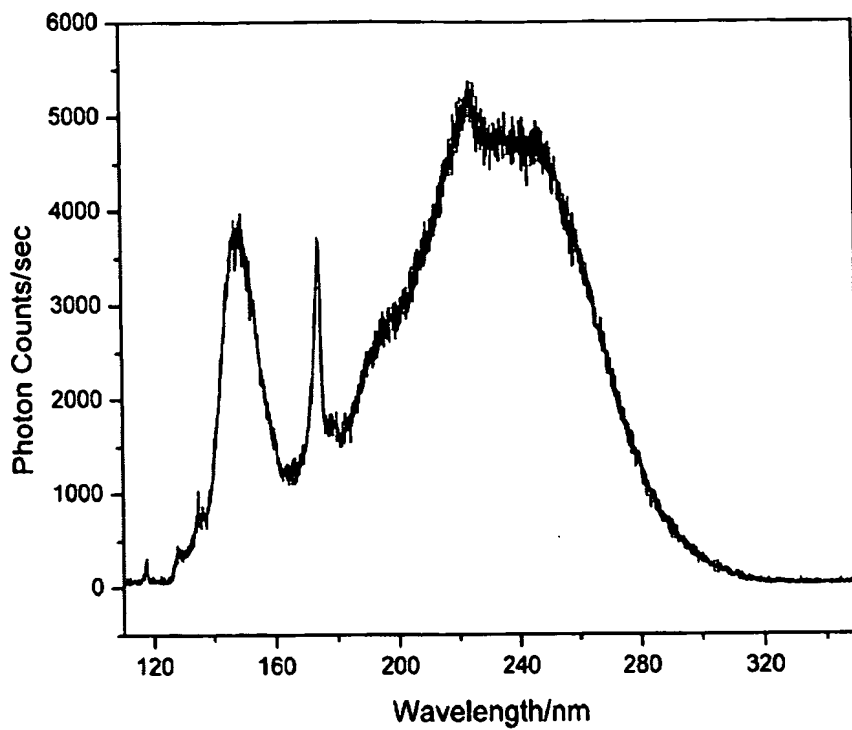


Fig. 1

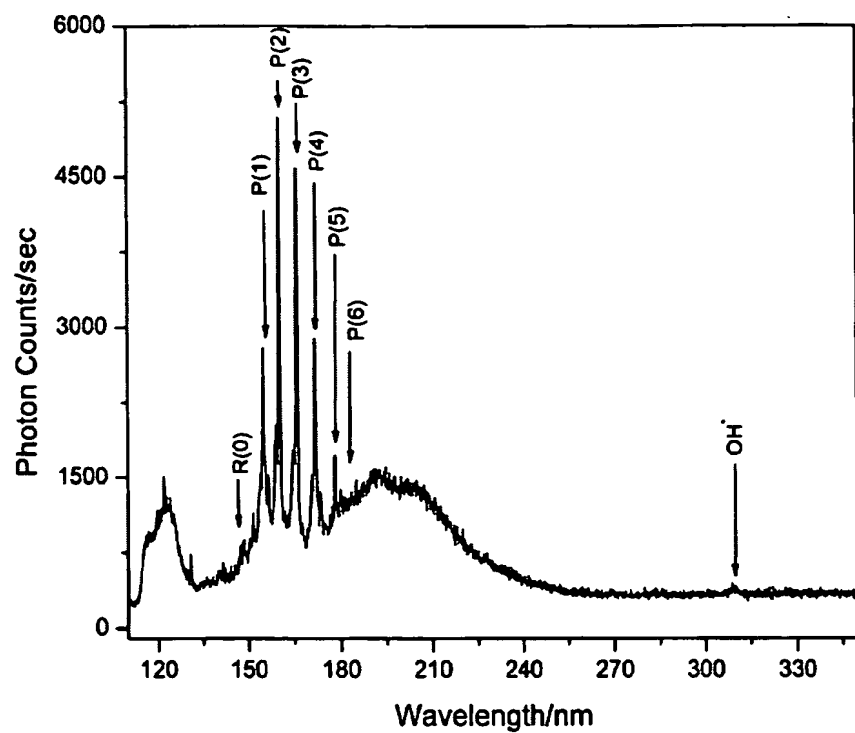


Fig. 2

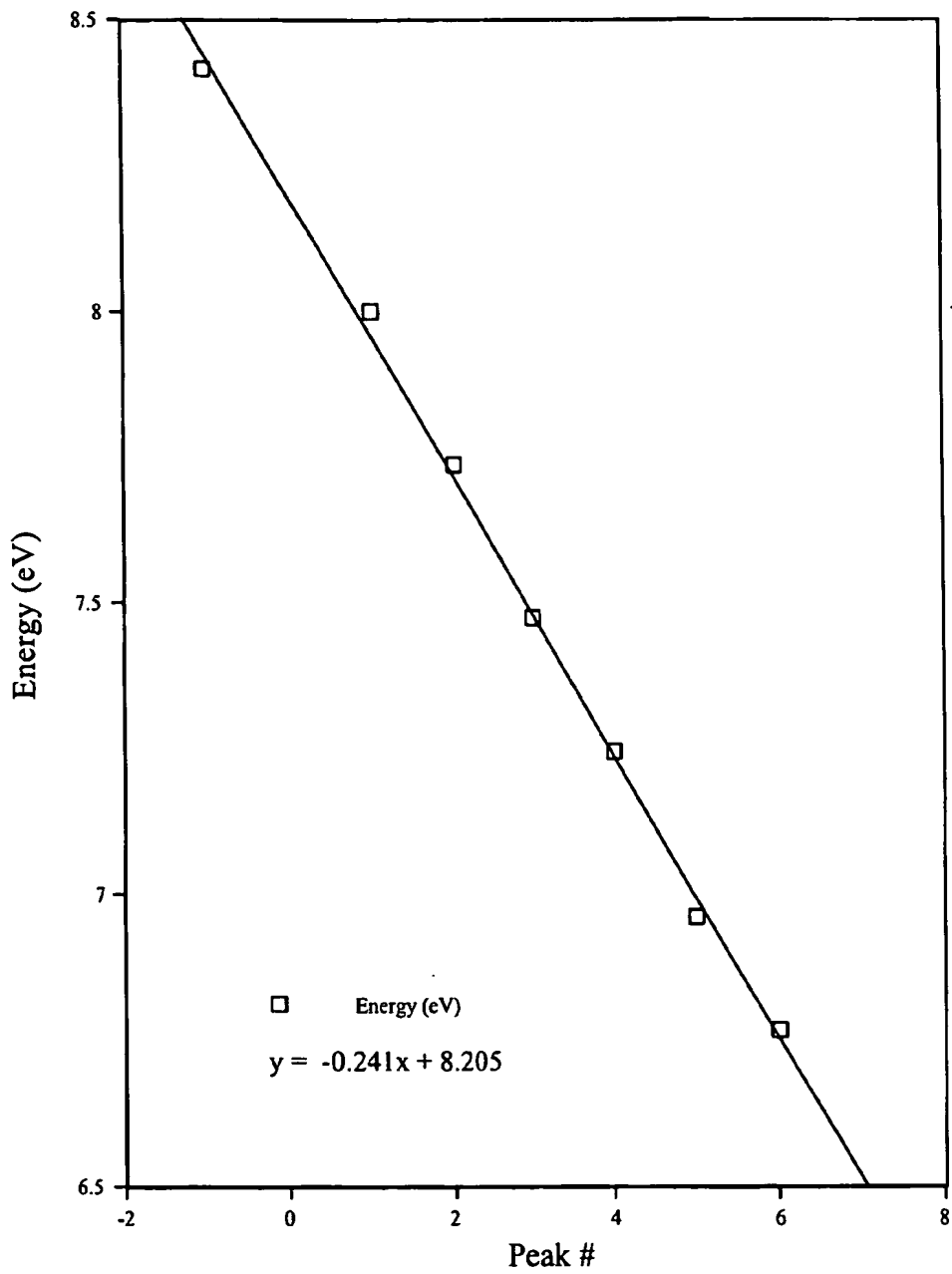


Fig. 3

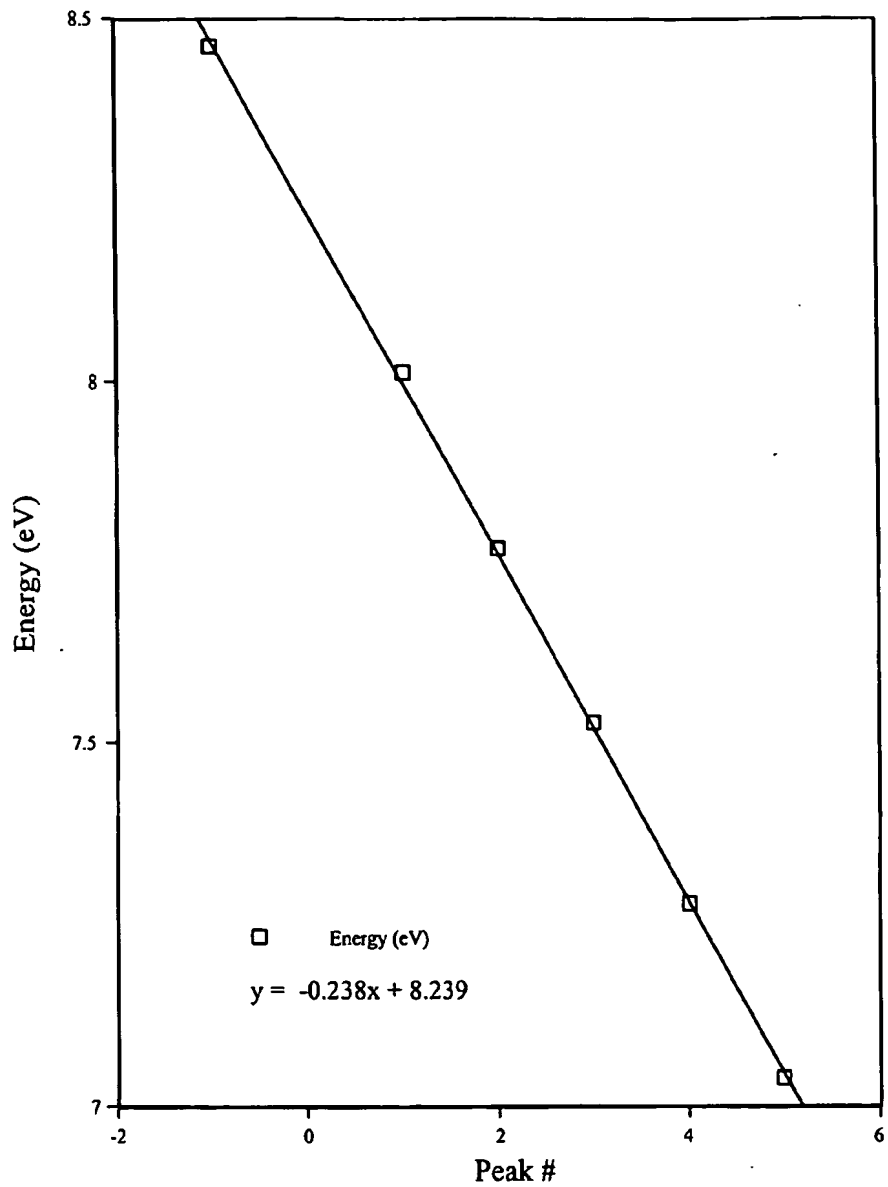


Fig. 4

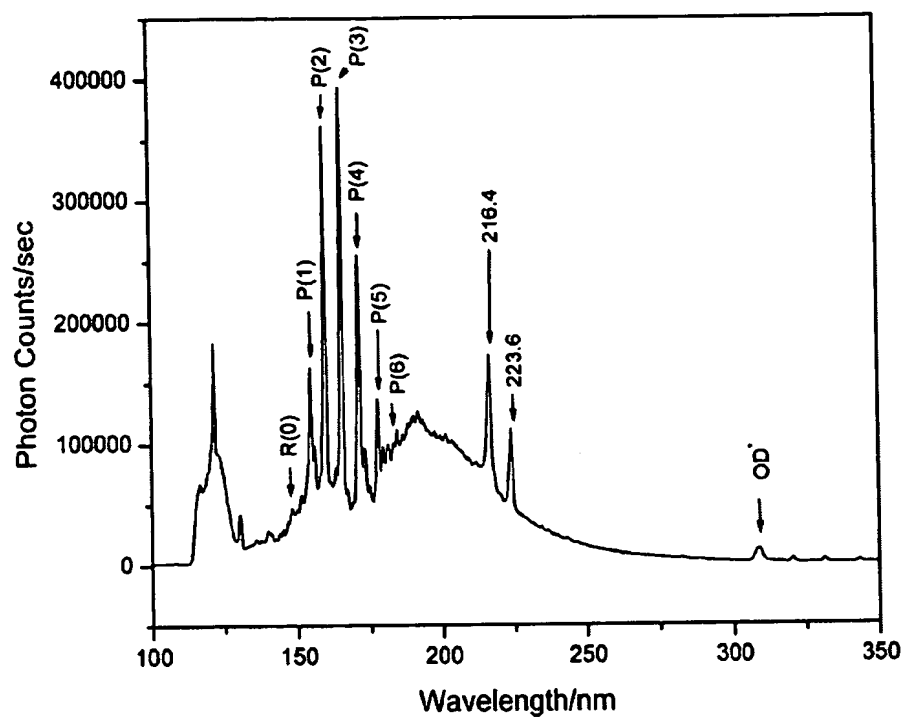


Fig. 5

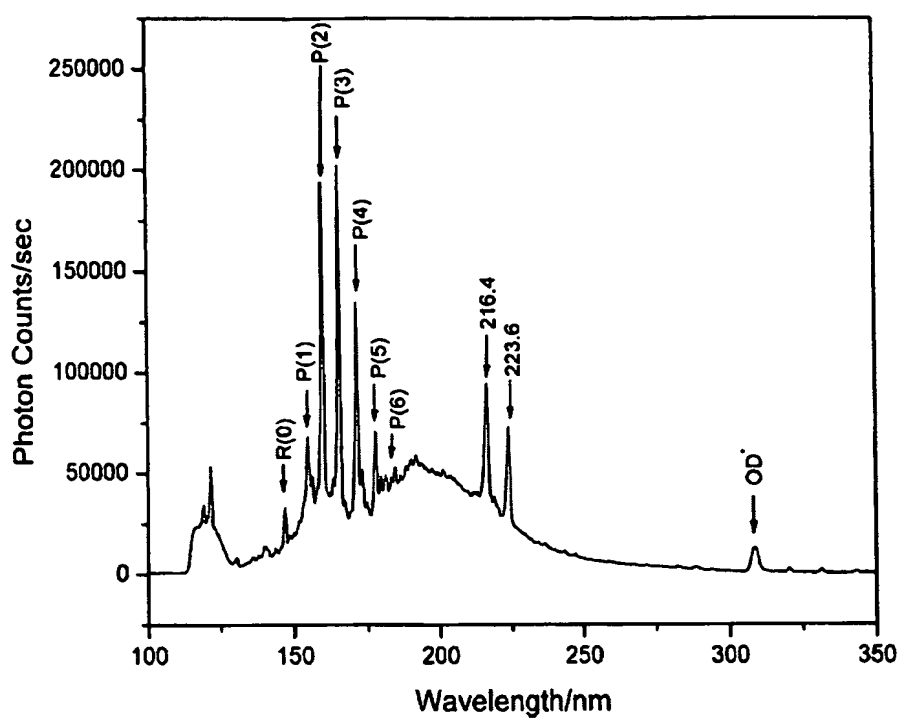


Fig. 6

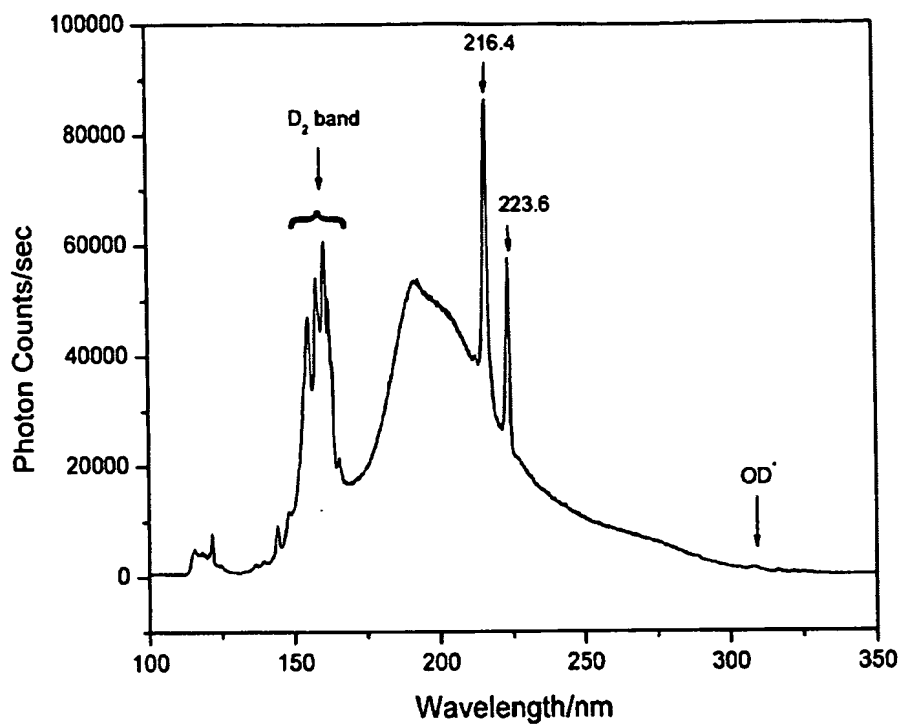


Fig. 7

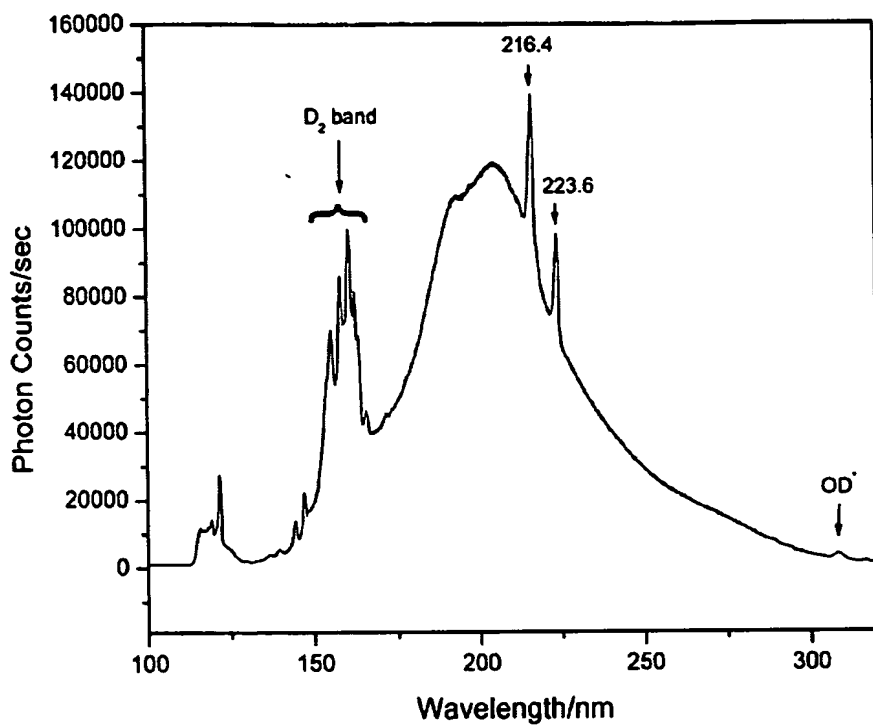


Fig. 8

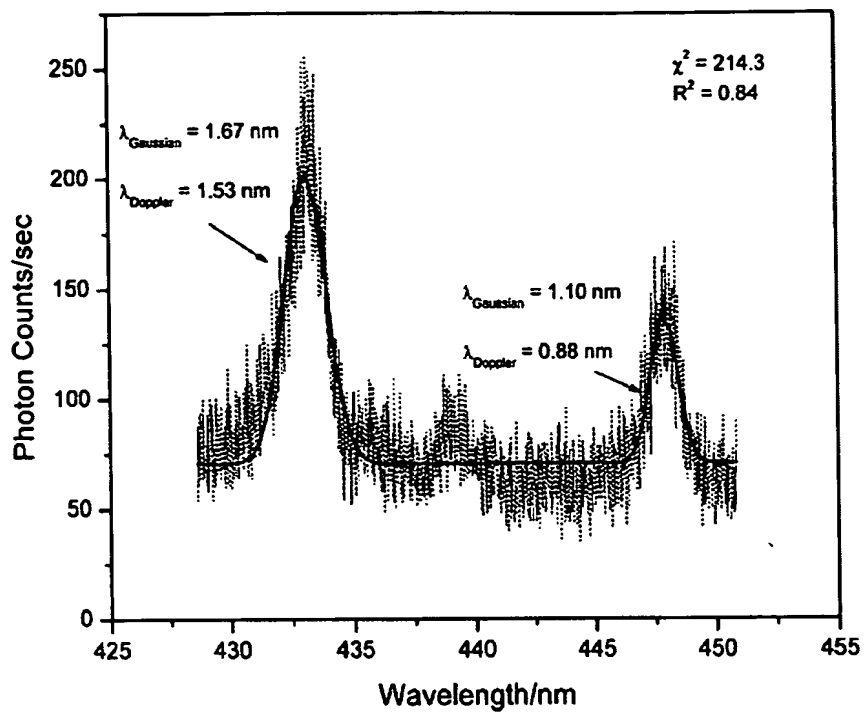


Fig. 9

Document made available under the Patent Cooperation Treaty (PCT)

International application number: PCT/US04/035143

International filing date: 22 October 2004 (22.10.2004)

Document type: Certified copy of priority document

Document details: Country/Office: US
Number: 60/546,174
Filing date: 23 February 2004 (23.02.2004)

Date of receipt at the International Bureau: 05 January 2005 (05.01.2005)

Remark: Priority document submitted or transmitted to the International Bureau in compliance with Rule 17.1(a) or (b)



World Intellectual Property Organization (WIPO) - Geneva, Switzerland
Organisation Mondiale de la Propriété Intellectuelle (OMPI) - Genève, Suisse